Heliyon 8 (2022) e09966

Contents lists available at ScienceDirect

Heliyon

journal homepage: www.cell.com/heliyon

Research article

Analytical study to determine the optical properties of gold nanoparticles in the visible solar spectrum

Lamia L.G. Al-mahamad *

Department of Chemistry, College of Science, Mustansiriyah University, Baghdad, Iraq

ARTICLE INFO

Keywords:
Gold nanoparticles
Relativistic effect
Photocatalyst
Dimethylamine borane
Hydrogen gas
Narrowing band gap

ABSTRACT

In this work the optical properties of the formed gold nanoparticles, that obtained upon reducing the gold(I):6-thioguanosine hydrogel by dimethylamine borane (DMAB) have been studied. The analytical measurements to calculate the optical band gap showed a significant narrowing in the optical band gap value (E_g). Tauc plot was used to estimate the optical band gap (Eg) with the direct and indirect allowed transitions, before and after the reducing process. Narrowing the band gap is very important to increase the efficiency of the semiconductor material as it leads to absorbing in the visible region of the solar spectrum.

1. Introduction

The high emission gases make a great change in the global climate and this was a motivation for the researchers to explore renewable and clean resources of energy supplies to decline the results of consumption the fossil fuel that forms 90% of the total world energy [1]. Several resources are available as alternative resources such as solar cell, wind, geothermal and hydropower, these resources are considered clean compared to the fossil fuel, however, there are some circumstances for each one of these resources [2]. Another energy source which is characterized as a clean, easily stored, and a promising energy source, is the hydrogen (H_2) fuel. H_2 is mainly produced from petroleum and natural gas, and recently, more attention has been paid to produce the hydrogen, as an alternative fuel resource, from different renewable sources, and the interest in H_2 production is increased rapidly. H_2 gas can produce from different solid storage resources such as B–N based compounds, and such materials can be considered as a good supplying to a renewable source for sustainable energy in the foreseeable future. Dimethylamine borane (DMAB) is one of B–N compounds that can produce one mole of H_2 gas/mole of DMAB in the presence of a suitable catalyst [3, 4, 5, 6]. The mechanism of the photocatalytic method is based on using the solar energy to provide a clean and a high energy in a short time, and this includes absorption photons that lead to excite the components of the reaction, and as a consequence, generates a new species such as radicals or making decomposition the entities of the reaction, and this process normally occurs with the assistance of a photocatalyst [7]. Different materials have been used as a catalyst to generate H_2 gas such as metal oxides [8], metal nitride [9], metal sulfides [10], and nanomaterials [11, 12]. Nanomaterials such as gold nanoparticles play a vital role as a catalyst solar cells, for example, by improving the capacity of the photo-absorption and decreasing the effect of the physical properties, via the incorporation of the localized surface plasmon resonance (SPR) in these materials, which leads to induce photo-charging effect by increasing the light absorption [13, 14]. Gold nanoparticles can be excited in the visible region of the solar spectrum due to the electron oscillations that confine in a limited area of the NPs which called as SPR. The size and the distribution size of the AuNPs, that use in the photocatalytic system, has an effect on the position and the width of the SPR band [15]. Gold nanoparticles (AuNPs) are normally used as catalysts by supporting on metal oxides, such as titania and ceria, and it was reported that, the catalytic efficiency of the AuNPs is highly dependent on the properties of the gold such as the morphology and the size [16]. Gold nanoparticles with a smaller size have a highly efficient activity compared to the larger one or to the gold atoms on a bulk metal, and this belongs to the high surface area in the small particles, in addition, to the low coordination number of these small NPs, which make them to be more active, and the reason is attributed mainly to increasing the number of such particles on the surface [17, 18]. Nucleosides and their derivatives are capable of self-assembling and forming different morphology via hydrogen bonding, such as G-quartet, ribbon, nanowires, etc. [19, 20, 21, 22] The multifunctional properties of these compounds have seen growing in their attention due to the important role of these materials in different applications such as nanotechnology, drug delivery, conductivity, and so on [23, 24, 25, 26]. Herein, the mechanism

* Corresponding author.
E-mail address: Lamia.Almahamad@yahoo.com.

https://doi.org/10.1016/j.heliyon.2022.e09966
Received 10 December 2021; Received in revised form 5 January 2022; Accepted 12 July 2022

action of AuNPs, that formed upon reducing the one dimensional polymer of gold hydrogel, as an efficient catalytic that can be activated in the visible region of the solar spectrum in the dehydrogenation reaction of the DMAB has been displayed. The method revealed the ability of AuNPs to narrow the value of the band gap energy at room temperature in solvent–free medium resulting increase the speed of the dehydrogenation reaction of DMAB. The work reflects the important properties of AuNPs as highly active nanostructures that could be exploited in different applications such as nanotechnology fields, solar cells, catalysts, etc.

2. Experimental

2.1. Preparation gold(I) hydrogel

The sample of Au(I) hydrogel was prepared according to our previous work [23], by equimolar equivalents reaction that occurred between Au(I) ions and 6-thioguanosine nucleoside in aqueous solution. Typically, 1 ml of the hydrogel was prepared by mixing the solution of $HAuCl_4$ (13 mg, 0.033 mmol), formed reduced with two equivalents of 2,2′-thiodiethanol, to the solution of 6-thioguanosine (10 mg, 0.033 mmol).

2.2. Kinetic measurements

The data obtained by monitoring time-dependent to indicate the location of the surface plasmon resonance (SPR) for the AuNPs, that formed after reducing the polymer of Au(I):6-thioguanosine hydrogel by using DMAB, were used in this study [27]. The data were carried out by achieving a kinetic study to measure the absorption by using a Cary 100 Bio UV-Vis spectrophotometer with a quartz cuvette at room temperature with a wavelength in the range of 200–600 nm.

2.3. The dehydrogenation reaction of DMAB

A typical sample of Au(I) hydrogel was prepared by drop-casting 2 μL of the gel into a clean silicon wafer, after leaving to dry in the air, the sample was exposed to DMAB (0.1–0.3 g) in solvent-free medium at room temperature for 1 h. The reaction occurred in a sealed glass Petra-dish [27].

2.4. Optical band gap (E_g) calculation

The optical band gap was obtained by plotting the incident photon energy *(hv) versus* the direct and indirect allowed transitions $(\alpha hv)^{1/n}$ by using Tauc-Menth plot [28].

3. Results and discussion

The optical band gap (E_g) of the semiconductor materials should be laid between 1.6-2.5 eV in order to absorb light in the visible region of the solar spectrum, such materials are described as a narrow band gap material, while semiconductor material with wide band gap (~3.2 eV) can only absorb light in the ultraviolet region. Accordingly, to increase the enhancement of conversion the sunlight energy with high efficiency, the absorption range must be extended to involve the regions from visible to infrared. This can only be done by either doping with some metal ions such as Fe^{+3}, Mn^{+2}, Cr^{+3}, etc., or by using semiconductor quantum dots (QDs) such as CdSe, CdS, etc., to enhance the sensitivity of the semiconductor materials in the visible region [29]. Au(I):6-thioguanosine hydrogel is a semiconductor compound with optical absorption 3.44 eV ($\lambda = 360$ nm). To increase the photocatalytic efficiency of this compound in the visible region, it was reduced by using DMAB in order to produce AuNPs, which showed a high activity as a catalyst and this was proved by the fast reaction with DMAB in solvent-free medium at room temperature within 1h.

3.1. Mechanism action of AuNPs in the photocatalytic reaction of DMAB

The dehydrogenation reaction of DMAB has occurred in the presence of AuNPs as a catalyst in solvent-free medium at room temperature within 70 min. The reaction was very fast and this resulted in a significant conversion of DMAB into cyclic amine-borane product $(Me_2NBH_2)_2$ in addition to generate hydrogen gas. This observation indicates that the transformation of the hydride from DMAB is the rate-determining step which leads to increase the efficiency of the dehydrogenation reaction of DMAB, also, the high speed of this reaction suggests that no intermediate structures of DMAB were formed, however, if the reaction was occurring at a temperature higher than the room temperature, then this can lead to change the rate of the hydride transfer from DMAB and produces a negligible conversion into the cyclic $(Me_2NBH_2)_2$ and in accordance with, intermediate structures of DMAB will be formed [30], and this can decrease the efficiency of the dehydrogenation reaction. It seems that the formed AuNPs act as an electron donor source that increases the efficiency of the dehydrogenation reaction [16], as the electrons in the 5d band can be excited by the natural light to transfer to the 6sp band. The long lifetime of these electrons compared to the electrons of the surface plasmon resonance (SPR) helps in the transition to the surface of the AuNPs [31]. It should be noted that, the presence of AuNPs is very essential to prevent the rapid recombination between the electrons and the holes, as it was reported that the time duration of the electron-hole separation, which depends on several factors such as the NPs size, the morphology, etc., is 10 ps, hence, AuNPs can play a vital role in suppressing the recombination process of electron-hole pair [32]. The electrons that transferred to the surface of the AuNPs can move to reduce the hydride ions into H_2 gas. On the other hand, the generated 5d band can contribute to the new formed structures of DMAB, cyclic amine borane $(Me_2NBH_2)_2$, that formed after reducing the Au(I) hydrogel [33]. From overall, the role of AuNPs as a catalyst in the dehydrogenation reaction of DMAB can be assigned to the interband transitions that formed upon electrons transferring between 5d and 6sp bands under the visible light, this band has a suitable energy (~1.84 eV) [34], corresponding to a red wavelength, to excite such transitions and make the AuNPs acting as an efficient photocatalyst in the dehydrogenation reaction. In fact, the optical properties of the gold in the visible region of the spectrum can be assigned to the relativistic effect which helps in reducing the gap between the 5d band and the Fermi level [35, 36]. The most common semiconductor photocatalyst that used in different applications is TiO_2, which has a large band gap between 3 eV to 3.2 eV, this titania is normally excited in the UV region and as a consequence, the electron transfers from the valence band (VB) to the conduction band (CB) which leads to form electron-hole pairs, however, the recombination between these electrons and holes makes this semiconductor less efficient, and in order to decrease this recombination, TiO_2 is doped with transition metal ions which facilitate transferring the electron to the surface of the photocatalyst and suppressed the electron-hole recombination. Another factor that could lead to increase the efficiency of titania, is to excite this photocatalyst in the visible region, numerous studies have been done to address this approach [37, 38]. This is the first report that has demonstrated the effective role of formed AuNPs, that produced by reducing the Au(I) hydrogel with DMAB, as a photocatalyst in the visible region of the solar spectrum which leads to produce the H_2 gas as a product from the dehydrogenation reaction of DMAB. Figure 1 displays a schematic for the proposed mechanism to generate H_2 gas by the dehydrogenation reaction of DMAB in the presence of AuNPs as a catalyst.

3.2. Analytical measurements to calculate the optical band gap (E_g)

Tauc plot [28] is normally used to indicate the band gap energy of the semiconductor materials. In the direct semiconductor materials, such as ZnO, GaN, etc., the conduction band, CB (which is above the band gap) and the valence band, VB (which is underneath the band gap) have the same momentum. While the value of momentum is different in the indirect semiconductor materials, such as Ge, Si, etc., for both states [29]. Plotting the $(\alpha hv)^{1/n}$ *versus* the *hv* gives the value of the E_g and the straight line can be extrapolated to the baseline of x axis to find the optical band gap. The spectrophotometric measurements that used for achieving

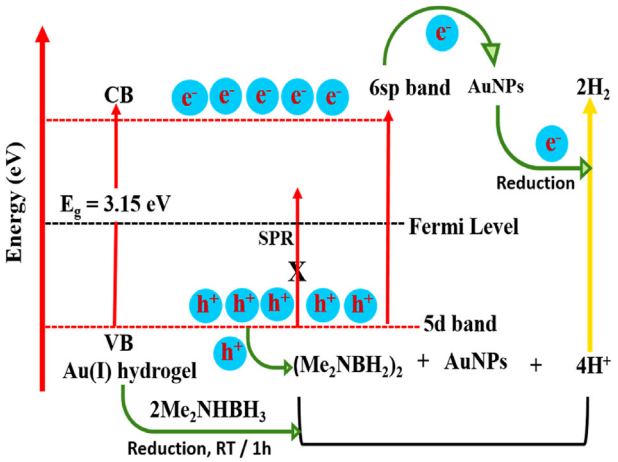

Figure 1. Schematic shows the proposed mechanism to generate H_2 gas by the dehydrogenation reaction of DMAB in the presence of AuNPs as a catalyst.

monitoring time-dependent to indicate the localized surface plasmon resonance (LSPR) were carried out by using Cary 100 Bio UV-Visible Spectrophotometer. The polymer of Au(I):6-thioguanosine hydrogel revealed a strong optical band at 360 nm (3.44 eV), that can be assigned to the charge transfer complex that formed between Au(I) ions and the nucleoside, 6-thioguanosine, via 6S [39], and upon reducing the polymer by using DMAB, a new band revealed at 530 nm (2.33 eV) which can attribute to the formation of the surface plasmon resonance band (SPR) for the formed AuNPs [40]. It is important to note that, the SPR band depends on several factors such as the environment surrounding the nanoparticles; and this factor influences through the optical index, and the higher SPR is related to the higher optical index, another factor is the morphological structure of the nanoparticles; as it was observed that the high symmetric nanoparticles normally have a blue shifted wavelength, and finally the core-shell particles; this factor effects when the size of NPs is larger than 60 nm due to the formation of a large SPR band that leads to shift the dipolar contribution [41]. A strong wavelength peak at 530 nm was observed with the peak formed after 30 min of the reduction with DMAB, and by increasing the reduction time a slight blue shift (~30 nm) was observed in this peak and this occurred as a consequence of the effect of quantum confinement, which confirms that, the strong absorption wavelengths be smaller with smaller NPs and longer with increasing the size, and this leads to produce high and low energy band gaps, respectively [42]. In addition to the emerging a slightly blue shift in the positions of the SPR bands after 30 min of reduction time, noticeably, a gradual decrease in the intensity of the absorption band can, also, be seen after 30 min of the reducing time and this may be attributed to the formation of an agglomeration in the formed NPs which led to decline the photocatalytic of AuNPs as a result of decrease both the surface area and the possibility to access into the active sites [3, 27]. Figure 2 (a) shows a kinetic study for monitoring time-dependent using UV-Vis spectroscopy of the formed AuNPs, the data display that the optimum time was to be 30 min. Also, the data reveal the location of the surface plasmon resonance (SPR) that formed after reducing Au(I) hydrogel at 530 nm, while Figure 2 (b) reveals that the dehydrogenation reaction of DMAB, that involves the formation of AuNPs and generates H_2 gas, follows the first-order kinetics, plotting the relation of ln A_0/A_t *versus* the reducing time yielded the rate constant (k), for this reaction which was equal to 0.0036 min^{-1}. A_0 and A_t, are the absorbance values at t = 0 and the optimum time (30 min), respectively.

3.3. The relationship between the band tail and sub band gaps

Tauc plot was used to determine the band gap energy (E_g) for the Au(I) hydrogel before and after reducing with DMAB within 70 min at room temperature, by plotting the energy of light (hv/eV) *versus* $(\alpha hv)^2$ (eV^2cm^{-2}) & $(\alpha hv)^{0.5}$ ($eV^{0.5}cm^{-0.5}$), for the direct and indirect allowed transitions, respectively. Extrapolating the straight line to the x axis produced the value of E_g. The data present in Figure 3 (a & b) reveals clearly the difference in the optical band gap energy values before and after reducing the sample, respectively, the reason can be assigned to the effect of AuNPs that formed after reducing the sample of Au(I) hydrogel with the DMAB. Before reducing the sample of the gel, the value of the optical band gap was 3.15 eV, and the optical absorption of the sample of the gel was 3.44 eV, however, upon reducing the sample of the gel with the DMAB, the value of E_g decreased to 2.45 eV, in addition, a new optical absorption band was formed at 2.33 eV corresponding to the surface plasmon resonance (SPR). It was reported that, the VB energy of the 5d band in AuNPs is 7.88 eV and the energy of the CB band of 6sp is 4.37 eV [33], and this means, the reduction potential of H^+/H_2 is less positive than the bottom of 6sp and the oxidation potential of DMAB is less negative than the top of 5d, and in accordance with, it seems that the locations of these bands are responsible for transferring the electrons and they clarify the ambiguity about the important role of AuNPs in the dehydrogenation reaction of DMAB. In addition, the presence of AuNPs can lead to broadening the valence band (VB) which results in narrowing the band gap. On the other hand, AuNPs can induce the formation of a strong band tail, however, such band tail was not found in the absence of AuNPs before the reducing process, as demonstrated in the direct and indirect allowed transitions in Figure 3 before reducing (a & c) and after reducing (b & d), respectively [14, 34, 43, 44]. It is worthy to note, the difference in the value of the band gap between the direct and the indirect allowed transitions for both the reactions, before and after, reduction. Direct transitions take place by interactions of photon-electron, while indirect transitions involve the incorporation of phonons in addition to the photons and electrons, and the type of the transition could be depending on the selection rules of quantum

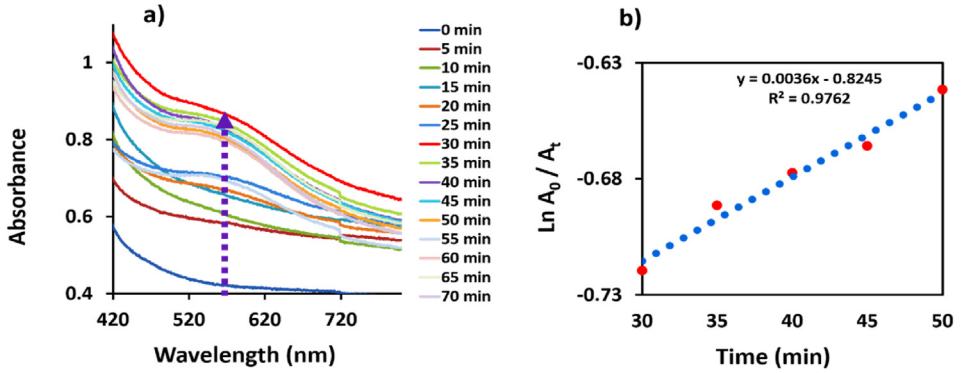

Figure 2. (a) Time-dependent UV-Vis spectroscopy kinetic study of the formed AuNPs showing the optimum time to be 30 min. (b) Plotting the relation of ln A_0/A_t versus the reducing time showed that the reaction follows the first-order kinetics and the rate constant (k) was 0.0036 min^{-1}.

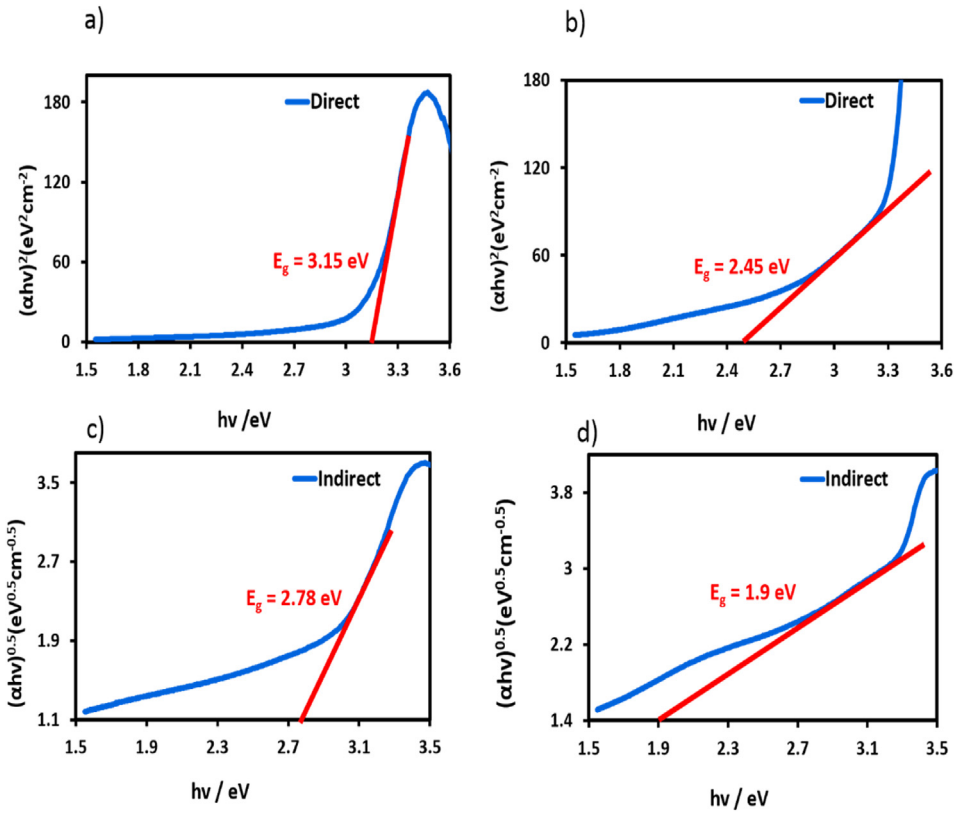

Figure 3. Tauc plot for determining the optical band gap (Eg) for Au(I) hydrogel with direct allowed transitions before and after reducing (a, b) and with indirect allowed transitions, before and after reducing (c, d), respectively. The data obtained with the optimum time (30 min).

mechanics in addition to the occupy and empty states of the electrons in the top of the valence band or conduction band, respectively. Normally, the direct transitions are combined with the emission or the absorption of the photons, while the probability of photon emission with indirect band gap semiconductor transitions is much lower because the wavenumber of the electrons (and therefore the momentum) is equal for direct transitions and its change for indirect transitions [45, 46]. The onset shape of the direct electronic transitions seems as a step, while that of the indirect band gap reveals with much gradual, and this could be assigned to the relationship between the shape of the transitions and their symmetries of the

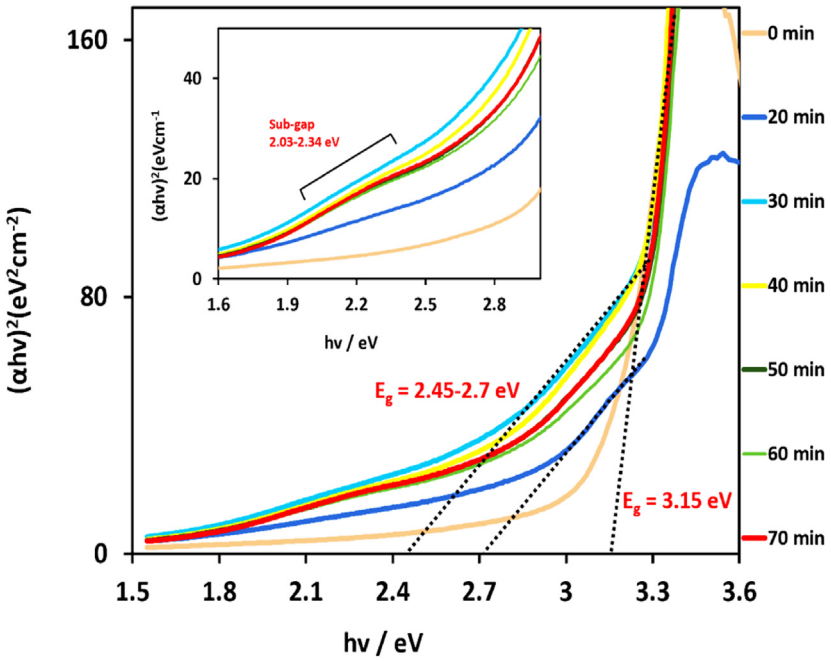

Figure 4. Determination of the band gap energy values (Eg) via direct allowed transitions using the Tauc plot for Au(I) hydrogel, that reduced by DMAB during a period of 0–70 min at room temperature, revealed narrowing in the band gap energy from 3.15 eV (before reducing) to 2.45–2.7 eV (after reducing). The inset shows the appearance of sub-gap bands in the range of 2.03–2.34 eV for the formed AuNPs after reducing within 70 min.

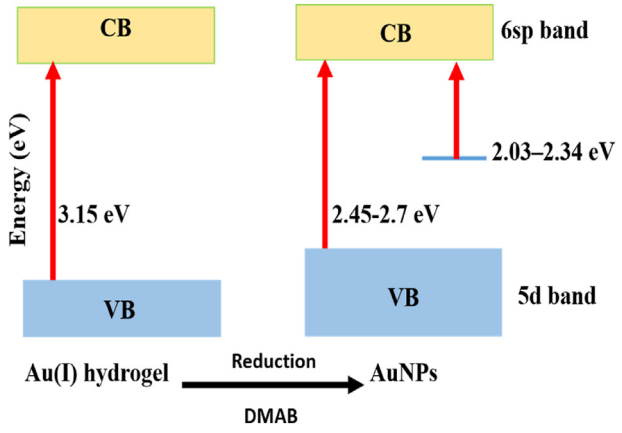

Figure 5. Schematic illustrating the possible changes that occurred in the value of the band gap energy (Eg) for the Au(I) hydrogel upon reducing by DMAB and forming AuNPs, the Eg value was narrowed from 3.15 eV to 2.45–2.7 eV by the influence of formation of AuNPs and broadening the VB band.

energy and the shape of the band gaps. This phenomena could indicate the nature of the compound if it has amorphous or crystalline properties [47]. Materials with direct allowed transitions can adsorb only photon energy without disturbing by adsorbing any phonon, and for this reason they have a potential for application in optoelectronic devices [48]. Also, the presence of indirect band gap with a smaller value compared to that for a direct band gap in the same compound leads to produce an efficient catalyst for achieving the excitation in the solar light and this can be attributed to the availability of sufficient phonons that help in the indirect transition of electrons from the valence band to the conduction band [49].

3.4. The effect of sub-gap bands on the efficiency of the photocatalyst

The appearance of a long tail in the fundamental band gap, which seems to be shifted to the red area of the energy level, can easily refer to the presence of a sub band-gaps [50, 51], This finding was consistent with the data collected from the kinetic study to monitor the progress in the reduction of Au(I) xerogel by DMAB at room temperature within a period of 70 min, as shown in Figure 4. The data display with more clearly emerging long bands tails that extending to the red area of the light energy level associated with the reducing time during the intervals from 20 min to 70 min, while such band tail has not been seen in the sample before starting the reduction process (pink colour line corresponding with interval l0 min in Figure 4). The inset in Figure 4 reveals the formation of the sub-gap bands covering the area from 2.03 eV to 2.34 eV [52]. In accordance with, the interval of energy between two levels will be $E_1 < E_2$, $E_2 < E_3$, etc. The significant sub band gap can be clearly observed in Figure 4. The emerging of sub band-gaps are very interesting in the materials that can narrow the band gap via direct allowed transitions as such properties can enhance the solar cell efficiency [53].

The variation in the band gap values after reducing the sample at different intervals time refers to the shift that occurred in the conduction and valence bands by the effect of AuNPs [14]. The schematic in Figure 5 shows the changing that occurred in the value of the band gap energy for the Au(I) hydrogel upon reducing with DMAB, as this value was narrowed from 3.15 eV to 2.45–2.7 eV due to the effect of AuNPs that formed after reducing the sample of the gel, also, the scheme shows the energy levels of the sub-band gaps and the broadening of the VB band that forms and lead to suppress the recombination of the electron-hole pairs and as a consequence increasing the catalytic efficiency of AuNPs.

4. Conclusions

In summary, the work principle of AuNPs as a high efficiency photocatalyst in dehydrogenation reaction of the DMAB to generate H_2 gas has been presented in this work. The photocatalytic process occurred in the visible light at room temperature in solvent-free medium. The formed AuNPs, that produced by reducing the Au(I) hydrogel by DMAB, play a vital role in the dehydrogenation reaction of the DMAB owing to the relativistic effect property in the gold, which helps in the formation of an interband as a result of transferring the electrons from 5d to 6sp. This band is responsible for the catalytic efficiency of the AuNPs in this reaction. In addition, the data that obtained by using Tauc plot revealed an important narrowing in the band gap energy after reducing the polymer of the gel with the DMAB, and this can be assigned to the effect of AuNPs which leads to broadening the valence band. Also, the presence of AuNPs suppresses the recombination between the electron-hole pairs which leads to increase the efficiency of AuNPs in the production of H_2 gas by transferring the electrons onto the surface of AuNPs then move to reduce the hydride ions. Interestingly, the reaction was very fast and the reduction occurred within 1h. It is worth to note that, the data showed formation of sub-band gaps after reducing the hydrogel, and formation of such sub band-gaps are very important in the development of the energies of solar cells.

Declarations

Author contribution statement

Lamia L. G. Al-mahamad: Conceived and designed the experiments; Performed the experiments; Analyzed and interpreted the data; Contributed reagents, materials, analysis tools or data; Wrote the paper.

Funding statement

This work was supported by Mustansiriyah University and the Iraqi Ministry of Higher Education and Scientific Research.

Data availability statement

Data included in article/supplementary material/referenced in article.

Declaration of interests statement

The authors declare no conflict of interest.

Additional information

No additional information is available for this paper.

References

[1] S.J. Davis, K. Caldeira, Consumption-based accounting of CO_2 emissions, Proc. Natl. Acad. Sci. USA 107 (12) (2010) 5687–5692.
[2] T. Jafari, E. Moharreri, A.S. Amin, R. Miao, W. Song, S.L. Suib, Photocatalytic water splitting—the untamed dream: a review of recent advances, Molecules 21 (7) (2016) 900.
[3] S. Karaboga, S. Özkar, Ceria supported ruthenium nanoparticles: remarkable catalyst for H2 evolution from dimethylamine borane, Int. J. Hydrogen Energy 44 (48) (2019) 26296–26307.
[4] C. Du, Q. Ao, N. Cao, L. Yang, W. Luo, G. Cheng, Facile synthesis of monodisperse ruthenium nanoparticles supported on graphene for hydrogen generation from hydrolysis of ammonia borane, Int. J. Hydrogen Energy 40 (18) (2015) 6180–6187.
[5] S. Akbayrak, S. Özkar, Ammonia borane as hydrogen storage materials, Int. J. Hydrogen Energy 43 (40) (2018) 18592–18606.
[6] U.B. Demirci, Ammonia borane, a material with exceptional properties for chemical hydrogen storage, Int. J. Hydrogen Energy 42 (15) (2017) 9978–10013.
[7] K. Takanabe, Transferring knowledge of electrocatalysis to photocatalysis: photocatalytic water splitting, in: M. Van de Voorde, B. Sels (Eds.), Nanotechnology in Catalysis, Wiley-VCH Verlag GmbH & Co. KGaA, 2017, pp. 891–906.
[8] K. Zhang, S. Qian, W. Kim, J.K. Kim, X. Sheng, J.Y. Lee, et al., Double 2-dimensional H 2 -evoluting catalyst tipped photocatalyst nanowires: a new avenue for high-efficiency solar to H 2 generation, Nano Energy 34 (2017) 481–490.
[9] J. Liu, J. Feng, J. Gui, T. Chen, M. Xu, H. Wang, et al., Metal@semiconductor core-shell nanocrystals with atomically organized interfaces for efficient hot electron-mediated photocatalysis, Nano Energy 48 (2018) 44–52.

[10] A. Agosti, Y. Nakibli, L. Amirav, G. Bergamini, Photosynthetic H2 generation and organic transformations with CdSe@CdS-Pt nanorods for highly efficient solar-to-chemical energy conversion, Nano Energy 70 (2020), 104510.

[11] T. Jafari, E. Moharreri, A.S. Amin, R. Miao, W. Song, S.L. Suib, Photocatalytic water splitting-the untamed dream: a review of recent advances, Molecules 21 (7) (2016).

[12] L. Guo, C. Zhong, J. Cao, Y. Hao, M. Lei, K. Bi, et al., Enhanced photocatalytic H2 evolution by plasmonic and piezotronic effects based on periodic Al/BaTiO3 heterostructures, Nano Energy 62 (2019) 513–520.

[13] H. Choi, W.T. Chen, P.V. Kamat, Know thy nano neighbor. Plasmonic versus electron charging effects of metal nanoparticles in dye-sensitized solar cells, ACS Nano 6 (5) (2012) 4418–4427.

[14] J. Villanueva-Cab, P. Olalde-Velasco, A. Romero-Contreras, Z. Zhuo, F. Pan, S.E. Rodil, et al., Photocharging and band gap narrowing effects on the performance of plasmonic photoelectrodes in dye-sensitized solar cells, ACS Appl. Mater. Interfaces 10 (37) (2018) 31374–31383.

[15] A. Primo, H. García, Chapter 6 - solar photocatalysis for environment remediation, in: S.L. Suib (Ed.), New and Future Developments in Catalysis, Elsevier, Amsterdam, 2013, pp. 145–165.

[16] J. Shi, On the synergetic catalytic effect in heterogeneous nanocomposite catalysts, Chem. Rev. 113 (3) (2013) 2139–2181.

[17] G.C. Bond, Introduction to the physical and chemical properties of gold, in: C.O. Louis Pluchery (Ed.), Gold Nanoparticles for Physics, Chemistry and Biology, Imperial College Press, 2012, pp. 171–197.

[18] G. Bond, T. David, Formulation of mechanisms for gold-catalysed reactions, Gold Bull. 42 (4) (2009) 247–259.

[19] L.L.G. Al-mahamad, Synthesis and surface characterization of new triplex polymer of Ag(I) and mixture nucleosides: cytidine and 8-bromoguanosine, Heliyon 5 (5) (2019), e01609.

[20] L.L.G. Al-mahamad, Gold nanoparticles driven self-assembling hydrogel via Host–Guest system, J. Mol. Struct. (2019), 127063.

[21] M. El Garah, R.C. Perone, A.S. Bonilla, S. Haar, M. Campitiello, R. Gutierrez, et al., Guanosine-based hydrogen-bonded 2D scaffolds: metal-free formation of G-quartet and G-ribbon architectures at the solid/liquid interface, Chem. Commun. (Camb) 51 (58) (2015) 11677–11680.

[22] L.L.G. Al-mahamad, Structure and Surface Texture Characterisation of Fibres and Nanoparticles in Silver(I):6-Guanosine Hydrogel, in: 2020 IEEE 10th International Conference Nanomaterials: Applications & Properties (NAP), 2020, pp. 1–6.

[23] L.L.G. Al-Mahamad, O. El-Zubir, D.G. Smith, B.R. Horrocks, A. Houlton, A coordination polymer for the site-specific integration of semiconducting sequences into DNA-based materials, Nat. Commun. 8 (1) (2017) 720.

[24] T. Bhattacharyya, P. Saha, J. Dash, Guanosine-derived supramolecular hydrogels: recent developments and future opportunities, ACS Omega 3 (2) (2018) 2230–2241.

[25] L. Stefan, D. Monchaud, Applications of guanine quartets in nanotechnology and chemical biology, Nat. Rev. Chem 3 (11) (2019) 650–668.

[26] O. El-Zubir, P.R. Martinez, G. Dura, L.L.G. Al-Mahamad, T. Pope, T.J. Penfold, et al., Circularly polarised luminescence in an RNA-based homochiral, self-repairing, coordination polymer hydrogel, J. Mater. Chem. C 10 (18) (2022) 7329–7335.

[27] L.L.G. Al-mahamad, Gold nanoparticles as a catalyst for dehydrogenation reaction of dimethylamine borane at room temperature, Int. J. Hydrogen Energy 45 (21) (2020) 11916–11922.

[28] J. Tauc, A. Menth, States in the gap, J. Non-Cryst. Solids 8–10 (1972) 569–585.

[29] N. Chouhan, R.-S. Liu, J. Zhang, Photochemical Water Splitting : Materials and Applications, 2017.

[30] V. Yempally, S. Moncho, Y. Wang, S.J. Kyran, W.Y. Fan, E.N. Brothers, et al., Thermal dehydrogenation of dimethylamine borane catalyzed by a bifunctional rhenium complex, Organometallics 38 (13) (2019) 2602–2609.

[31] E. Khon, A. Mereshchenko, A.N. Tarnovsky, K. Acharya, A. Klinkova, N.N. Hewa-Kasakarage, et al., Suppression of the plasmon resonance in Au/CdS colloidal nanocomposites, Nano Lett. 11 (4) (2011) 1792–1799.

[32] M.A. Mahmoud, W. Qian, M.A. El-Sayed, Following charge separation on the nanoscale in Cu(2)O-Au nanoframe hollow nanoparticles, Nano Lett. 11 (8) (2011) 3285–3289.

[33] B. Tian, Q. Lei, B. Tian, W. Zhang, Y. Cui, Y. Tian, UV-driven overall water splitting using unsupported gold nanoparticles as photocatalysts, Chem. Commun. (Camb) 54 (15) (2018) 1845–1848.

[34] W. Chamorro, J. Ghanbaja, Y. Battie, A.E. Naciri, F. Soldera, F. Mücklich, et al., Local structure-driven localized surface plasmon absorption and enhanced photoluminescence in ZnO-Au thin films, J. Phys. Chem. C 120 (51) (2016) 29405–29413.

[35] G.C. Bond, Introduction to the physical and chemical properties of gold, in: C. Louis, O. Pluchery (Eds.), Gold Nanoparticles for Physics, Chemistry and Biology, Imperial College Press, 2012, pp. 29–49.

[36] P. Pyykko, Relativistic effects in structural chemistry, Chem. Rev. 88 (3) (1988) 563–594.

[37] R. Rahal, S. Daniele, L.G. Hubert-Pfalzgraf, V. Guyot-Ferréol, J.-F. Tranchant, Synthesis of para-amino benzoic acid–TiO2 hybrid nanostructures of controlled functionality by an aqueous one-step process, Eur. J. Inorg. Chem. 2008 (6) (2008) 980–987.

[38] W. Xie, R. Li, Q. Xu, Enhanced photocatalytic activity of Se-doped TiO2 under visible light irradiation, Sci. Rep. 8 (1) (2018) 8752.

[39] E.J. Fernandez, A. Laguna, J.M. Lopez-de-Luzuriaga, M. Monge, E. Sanchez-Forcada, Different phosphorescent excited states of tetra- and octanuclear dendritic-like phosphine gold(I) thiolate complexes: photophysical and theoretical studies, Dalton Trans. 40 (13) (2011) 3287–3294.

[40] V. Amendola, R. Pilot, M. Frasconi, O.M. Marago, M.A. Iati, Surface plasmon resonance in gold nanoparticles: a review, J. Phys. Condens. Matter 29 (20) (2017), 203002.

[41] O. Pluchery, Optical properties of gold nanoparticles, in: C. Louis, O. Pluchery (Eds.), Gold Nanoparticles for Physics, Chemistry and Biology, Imperial College Press, 2012, pp. 43–73.

[42] J. Wang, L. Wei, L. Zhang, C. Jiang, E. Siu-Wai Kong, Y. Zhang, Preparation of high aspect ratio nickel oxide nanowires and their gas sensing devices with fast response and high sensitivity, J. Mater. Chem. 22 (17) (2012) 8327.

[43] D. Sahu, N.R. Panda, B.S. Acharya, A.K. Panda, Enhanced UV absorbance and photoluminescence properties of ultrasound assisted synthesized gold doped ZnO nanorods, Opt. Mater. 36 (8) (2014) 1402–1407.

[44] N. Serpone, Is the band gap of pristine TiO2 narrowed by anion- and cation-doping of titanium dioxide in second-generation photocatalysts? J. Phys. Chem. B 110 (48) (2006) 24287–24293.

[45] H.H. Wieder, Chapter 4 - optical properties, in: H.H. Wieder (Ed.), Intermetallic Semiconducting Films, Pergamon, 1970, pp. 197–229.

[46] R.J. Martín-Palma, J.M. Martínez-Duart, Chapter 3 - review of semiconductor physics, Nanotechnol. Microelectron. Photon. (2017) 51–80, second ed. Elsevier.

[47] N.J. Hilfiker, T. Tiwald, Dielectric function modeling, in: H. Fujiwara, Robert W. Collins (Eds.), Spectroscopic Ellipsometry for Photovoltaics. Volume 1: Fundamental Principles and Solar Cell Characterization, Springer Nature Switzerland, 2018, pp. 115–153. Chapter 5.

[48] W.G. Lee, S. Chae, Y.K. Chung, W.S. Yoon, J.Y. Choi, J. Huh, Indirect-to-direct band gap transition of one-dimensional V2Se9: theoretical study with dispersion energy correction, ACS Omega 4 (19) (2019) 18392–18397.

[49] N. Saha, A. Sarkar, A.B. Ghosh, A.K. Dutta, G.R. Bhadu, P. Paul, et al., Highly active spherical amorphous MoS2: facile synthesis and application in photocatalytic degradation of rose bengal dye and hydrogenation of nitroarenes, RSC Adv. 5 (108) (2015) 88848–88856.

[50] G. Rey, G. Larramona, S. Bourdais, C. Choné, B. Delatouche, A. Jacob, et al., On the origin of band-tails in kesterite, Sol. Energy Mater. Sol. Cell. 179 (2018) 142–151.

[51] J.K. Katahara, H.W. Hillhouse, Quasi-Fermi level splitting and sub-bandgap absorptivity from semiconductor photoluminescence, J. Appl. Phys. 116 (17) (2014), 173504.

[52] R.J. Martín-Palma, J.M. Martínez-Duart, Chapter 4 - basic properties of low-dimensional structures, in: R.J. Martín-Palma, J.M. Martínez-Duart (Eds.), Nanotechnology for Microelectronics and Photonics, second ed., Elsevier, 2017, pp. 81–105.

[53] Y. Wang, H.X. Ge, Y.P. Chen, X.Y. Meng, J. Ghanbaja, D. Horwat, et al., Wurtzite CoO: a direct band gap oxide suitable for a photovoltaic absorber, Chem. Commun. (Camb) 54 (99) (2018) 13949–13952.